Effects of surface pretreatments on interface structure during formation of ultra-thin yttrium silicate dielectric films on silicon

J. J. Chambers
Department of Chemical Engineering, North Carolina State University, Raleigh, NC 27695

B. W. Busch, W.H. Schulte, T. Gustafsson and E. Garfunkel
Departments of Physics and Chemistry, Rutgers University, Piscataway, NJ 08854

S. Wang and D. M. Maher
Department of Materials Engineering, North Carolina State University, Raleigh, NC 27695

T. M. Klein
Department of Chemical Engineering, University of Alabama, Tuscaloosa, AL 35487

G. N. Parsons[a]
Department of Chemical Engineering, North Carolina State University, Raleigh, NC 27695

X-ray photoelectron spectroscopy (XPS) and medium energy ion scattering (MEIS) are used to determine chemical bonding and composition of ultra-thin films of mixed yttrium, silicon, and oxygen, formed by oxidation of metal on clean and pre-treated silicon. XPS and MEIS analyses indicate that oxidation of yttrium on bare silicon results in a fully oxidized film with a significant fraction of Y-O-Si bonding. The mixed Y-O-Si structure results from the relatively rapid reaction between Y and the Si substrate to form yttrium silicide, followed by oxidation. The effect of various silicon pretreatments, including *in situ* oxidation and nitridation, on bulk and interface film composition are also examined. Transmission electron microscopy (TEM) of 40Å thick films indicates that the yttrium silicate films are amorphous with uniform contrast throughout the layer. MEIS shows evidence for a graded metal concentration in the dielectric near the silicon interface, with uniform oxygen concentration (consistent with full oxidation) throughout the film. Angle resolved XPS (ARXPS) shows no significant signal related to Si^{+4}, as would be expected from a substantial SiO_2 interface layer. Capacitance-voltage analysis demonstrates that a ~10 Å equivalent oxide thickness can be achieved. The effects of ultra-thin silicon oxide, nitrided-oxide and nitrided silicon interfaces on silicon consumption during the oxidation of yttrium are investigated. When yttrium is deposited on a thin (~10 Å) SiO_2 film and oxidized, a yttrium silicate film is formed with bonding and composition similar to films formed on bare silicon. However, when the interface is a thin nitride, the silicon consumption rate is significantly reduced, and the resulting film composition is closer to Y_2O_3. The consumption of the silicon substrate by metal is shown to occur during oxidation and during vacuum annealing of yttrium on silicon. The relatively rapid formation of metal-silicon bonds suggests that metal-silicon structures may also be important reactive intermediates in silicon/dielectric interface formation reactions during chemical vapor deposition. In addition to thermodynamic stability, understanding the relative rates of elementary reaction steps in film formation is critical to control composition and structure at the dielectric/Si interface.

[a)]electronic mail: parsons@ncsu.edu

Understanding bonding structure and defects at semiconductor/dielectric interfaces is a critical problem for applications in silicon field effect transistors, and the need for high dielectric constant (high-k) gate insulators makes the interface problem even more complex and challenging. Current attention is being placed on chemistry required to control interface bonding and reactivity during high-k deposition and during post-deposition processing. As transistor size is decreased, the thickness of the silicon dioxide gate dielectric must also decrease to maintain channel capacitance. However, the physical limits for the thin silicon dioxide, including the allowable leakage current due to quantum mechanical tunneling and oxide reliability, are rapidly being approached.[1,2] The exact limit will vary with the device application (i.e. low-power or high-performance), but current estimates for a lower limit of a 10-20 Å silicon dioxide place the insertion point for high-k dielectrics somewhere near the 100-65 nm nodes.[1] Since the capacitance scales as the dielectric constant over thickness, high-k materials should allow a thicker dielectric (compared to silicon dioxide) to combat tunneling, while maintaining sufficient capacitance to enable high channel transconductance.

High-k materials, including Y_2O_3,[3] Ta_2O_5,[4] TiO_2,[5] HfO_2,[6] ZrO_2[7] and Al_2O_3,[8] are currently being investigated as replacements for silicon dioxide. Unfortunately, chemical vapor deposition (CVD) and physical vapor deposition (PVD) of these high-k dielectrics often results in lower-k interface layers[4,9,10] that form due to unwanted silicon substrate consumption.[11] Thermodynamic stability between the bulk metal oxide and silicon, such as Al_2O_3/Si,[12] does not alone preclude interface reactions from occurring. For example, the initial monolayers formed during metal-organic CVD of a metal oxide on silicon may proceed by breaking a metal-ligand bond, chemisorption of the metal complex (possibly involving a metal-silicon bond) and subsequent oxidation of the resulting intermediate complex. It is reasonable to assume that if metal-silicon bonds form as reactive intermediates then their oxidation will be an important step in interface layer formation. In order to control or eliminate unwanted interface layer formation, silicon nitride and silicon oxy-nitride engineered interfaces have been used to inhibit reaction with the substrate during high-k deposition. Integration of high-k dielectrics with existing silicon technology will require an understanding of interface layer formation including effects of potential reactive intermediate surface complexes, and engineered interfaces on silicon consumption.

In this work, we have used X-ray photoelectron spectroscopy and medium energy ion scattering to investigate silicon consumption during oxidation of yttrium on bare and *in situ* modified silicon. We report that oxidation of yttrium deposited on bare silicon results in mixing of yttrium and silicon to form yttrium silicate. Similar results are also obtained when the surface is oxidized silicon. However, when the silicon surface is nitrided prior to yttrium deposition, oxidation creates a structure closer to pure metal oxide consistent with the nitrided silicon impeding reaction with the substrate.

II. Experimental

The samples used were Si(100) p-type with resistivity 0.1-0.3 Ω-cm cut from commercial wafers into 2.5 X 2.5 cm^2 substrates. The "bare Si" samples were prepared by dipping for 5 minutes in JTB 100 (a tetramethylammonium hydroxide based alkaline solution with a carboxylate buffer), rinsing in deionized water (DI), etching in buffered hydrogen fluoride (HF) for 30 seconds with no final rinse and immediately loading into vacuum. Thermal (40 Å) SiO_2 substrates were cleaned prior to yttrium deposition by dipping for 5 minutes in JTB 100, rinsing in DI and immediately loading into vacuum.

Yttrium sputtering and vacuum annealing were performed in the system described in detail elsewhere.[13] A cylindrical plasma source on the processing chamber can be configured to run in a remote plasma mode to perform *in situ* silicon surface pretreatments and in a direct plasma mode to sputter yttrium thin films. The thickness of very thin yttrium films was determined from a calibrated sputter deposition rate, determined from step profilometry measurements of several thick (>100Å) films. Plasma oxidation and nitridation were used to form silicon surface pretreatments at 300°C, 50 mTorr, a radio frequency (rf) power of 400 W in 100 sccm (N_2) N_2O and N_2, respectively. The processing chamber is equipped with a retractable yttrium (99.1%, Ta is the major impurity) sputter target that can be isolated from the system by a gate valve. The sputter target was isolated from the processing chamber during the silicon surface pretreatment. Sputtering was performed at room temperature in 4.3 mTorr Ar, with rf power of 420W and a yttrium target dc bias of –1000V. The sputter rate was 25Å/minute and was monitored using the target current (3.4 mA). Annealing was performed in vacuum better than $5x10^{-6}$ Torr at 600°C for 2 minutes in the same chamber as the yttrium deposition. A standard 10cm diameter tube furnace was used for *ex situ* oxidation at temperatures from 600-900 °C in 1 atm. N_2O or air.

The following experiments were designed to investigate how silicon surface pretreatments affect silicon consumption. Yttrium (25 Å) was sputtered onto the following surfaces:

(1) bare (HF last) silicon

(2) 20 minute plasma oxidized silicon

(3) 20 minute plasma oxidized silicon followed by 10 minute plasma nitridation

(4) 20 minute plasma nitrided silicon.

The samples were then subjected to oxidation in 1 atm. N_2O at 600 °C for 2 minutes. The plasma silicon surface pretreatments were grown in the same vacuum chamber as the yttrium deposition.

X-ray photoelectron spectroscopy (XPS) was performed *ex situ* using a Riber LAS3000 equipped with a MAC2 analyzer (single-pass cylindrical mirror analyzer with an input lens) and an Mg Kα ($h\nu$ = 1253.6 eV) non-monochromatic X-ray source. Detailed spectra were collected at a take-off angle of 90° and a 0.1 eV step size. The raw spectra were smoothed using an eleven point Savitsky-Golay algorithm. When peak fitting was necessary to locate peak position or integrate area, Gaussian functions were generated by minimizing the misfit error. Charging of the samples was typically observed, which resulted in peak shifting by 1-2eV from expected positions. For thin samples, spectra were shifted to align both the adventitious carbon features near 285 eV and the Si 2p substrate peak at 99.3 eV. For every sample studied, these two peaks could be aligned to their expected positions using a constant peak shift value. For thicker samples, the adventitious carbon peak was used as a reference.

Angle resolved XPS was performed *ex situ* using a Kratos Axis 165 and Al Kα ($h\nu$ = 1486.6 eV). The resolution was ~ 0.8 eV, and the spot size was 120 μm. The step size was 0.1 eV and the take-off angle was varied from 20° to 90° in 10° increments. The angle resolved XPS data were not smoothed. The mean free path for Si 2p photoelectrons is approximately 25 Å, and sufficient intensity is expected throughout the films studied here (~40 Å) to observed bonding in the entire yttrium silicate.

Medium-energy ion scattering (MEIS),[14] a low-energy (50-300 keV) high depth resolution (~5 Å) version of Rutherford backscattering spectroscopy, was performed *ex situ* to obtain proton

energy spectra. Energy spectra of the scattered protons (~100 keV) are collected using a double-aligned geometry. The energy spectra are converted to a density versus depth scale using a kinematic factor calculated within a binary collision model along with tabulated electronic stopping[15] and straggling[16] values. The compositions determined by MEIS of the films reported here as average values up to a depth of ~20 Å and generally correspond to $(Y_2O_3)_x \cdot (SiO_2)_{1-x}$ where x ranged from 0.32 to 0.79. The known yttrium silicates correspond to x = 0.33 (keiviite) and x = 0.5 (yttrium orthosilicate).[17] The term "silicate" generally refers to crystalline materials with known composition. The films reported here are amorphous (based on TEM, RHEED and X-ray analyses) binary alloys, but because of the predominance of Y-O-Si bonds, rather than phase separated Y_2O_3/SiO_2 mixtures, the films are referred to as yttrium silicate, or simply Y-O-Si.

Metal-insulator-semiconductor capacitors were formed by evaporating 2000 Å of Al onto blanket yttrium silicate films through a contact mask with holes ranging from 50-500 μm in diameter. Active area was determined using scanning electron microscopy. Samples underwent a post-metallization anneal in 90% N_2 and 10% H_2 at 400 °C for 30 minutes. Capacitance-voltage (C-V) measurements were taken at 1 MHz using a HP 4284a LCR meter. Electrical thickness is described as an equivalent SiO_2 thickness (EOT) determined from a fit of the C-V curve that includes the quantum mechanical effect. Samples were swept from inversion to accumulation in the dark with no initial light source.

III. Results and Discussion

A. Oxidation of yttrium on silicon to form yttrium silicate films

To form ultra-thin dielectric layers, very thin yttrium films (as thin as ~8 Å) were deposited on silicon and oxidized at 900°C in N_2O for 15 seconds. The XPS analysis of an oxidized 8Å Y film is presented in the Y 3d, Si 2p and O 1s spectra of Fig. 1. The Y 3d spectrum of Fig. 1a exhibits a doublet resulting from the spin-orbit splitting of the Y $3d_{3/2}$ and Y $3d_{5/2}$ peaks at 160.8 and 159.0 eV, respectively, whereas the reference peak positions for Y $3d_{3/2}$ and Y $3d_{5/2}$ for Y_2O_3 are 158.8 and 156.8 eV,[18] respectively. The two peaks at 154 and 151 eV in the Y 3d spectrum result from a combination of the Y 3d satellite, Si-O Si 2s and substrate Si 2s peaks. Peaks assigned to the silicon substrate (99.3 eV) and Si-O bonding (102.9 eV) are observed in the Si 2p spectrum of Fig. 1b. The measured Si-O peak maximum is at lower binding energy than expected for SiO_2 (103.3 eV), and within the expected range (102-103 eV)[18] for Si-O bonding in metal silicates. The Si-O peak is broad (full-width-half-maximum (FWHM) = 2.4 eV, compared to a measured Si-O peak FWHM = 1.8 eV for SiO_2) consistent with a wide range of bonding environments available to silicon. No peaks for Y-Si at ~0.2 and ~0.6 eV lower than the metallic yttrium and silicon peaks, respectively, are observed in the Y 3d or Si 2p spectra. The O 1s peak (Fig. 1c) (broad peak with FWHM = 3.0 eV compared to a measured O 1s FWHM = 1.8 eV for SiO_2) is measured at 532.8 eV and is near O 1s for SiO_2 (533.0 eV). The broad peak is assigned to contributions from yttrium silicate (at energies between O 1s for SiO_2 and Y_2O_3 (529.5 eV)).

Figure 2a presents the corresponding MEIS proton energy spectrum for this yttrium silicate film. In agreement with the XPS spectra of Fig. 1, peaks for yttrium (~96 keV), silicon (~86.5 keV) and oxygen (~80.5 keV) are observed. The silicon peak at ~86 keV exhibits a shoulder at ~87 keV, which is assigned to silicon in the yttrium silicate film. Thickness obtained from MEIS depth profiles is based on the proton stopping power. Since precise values for the stopping power in Y-Si-O alloys have not been reported, we applied Bragg's Rule, where the stopping power is calculated from the stopping power of the components of the alloy. Such estimates are generally accurate

within 10-20%. However, a more accurate thickness can be obtained from the absolute areal densities of the atomic film constituents measured by MEIS. The integral yield of the yttrium peak in Fig. 2a corresponds to 1.83×10^{15} atoms/cm^2 (accuracy about ±5%). From the Y and deconvolved Si peak height (i.e. near surface Si yield) in Fig. 2a, the yttrium to silicon ratio is estimated to be approximately 1 to 1 within the first 15 Å of the surface (as shown in Fig. 2b). Fits to the data in Fig. 2a also indicate the total oxygen areal density in the dielectric film to be 15×10^{15} atoms/cm^2. Presuming that the mixed Y/Si layer is completely oxidized (which is consistent with the MEIS and XPS data in Figs. 1 and 2) the oxygen yield is consistent with excess oxygen in the dielectric layer. The amount of excess oxygen is equivalent to the amount of oxygen in a uniform SiO_2 layer that is 14 Å thick. However, because of uncertainty in the proton energy loss straggling, the yttrium profile near the interface cannot be determined precisely. As discussed below, angle resolved XPS results in Figure 3 do not show clear evidence for interfacial SiO_2, suggesting that more detailed analysis is required to unambiguously determine interface bonding composition in these dielectrics. Two possible yttrium profiles, determined from fits to data in Figure 2a, are shown schematically in Fig. 2b. Based on the XPS and electrical results, in Figs. 1 and 5, a graded Y profile at the interface is more likely. Further support for a graded profile is shown in the TEM in Fig. 4, since an abrupt profile would result in contrast, which is not observed in this TEM image. This indicates that the interface structure is more likely a graded silicate, with more silicon dioxide-rich composition at the interface. Under some processing conditions (i.e. thinner starting layers or longer oxidation times), films with a two layer structure can clearly be seen in the TEM images.

The bonding in yttrium silicate films was investigated as a function of depth using angle resolved XPS. Figure 3 presents the angle resolved XPS spectrum for a film formed by oxidizing a ~25 Å yttrium film on silicon at 900 °C for 2 minutes. The take-off angle is changed from 20° to 90° from grazing to normal incidence in order to probe the near surface and substrate/dielectric interface, respectively. The Y $3d_{5/2}$ peak in Fig. 3a remains fixed at 159.6 eV for take-off angles from 20° to 90°. The silicon substrate peak (99.3 eV) in Fig. 3b is observed to increase in magnitude as the take-off angle is varied from 20° to 90° consistent with the increased depth probed at normal incidence. Since the Si substrate peak is observed in the spectra, the Si/dielectric interface region is also probed. The Si-O feature (103.4 eV) in Fig. 3b remains fixed at 103.4 eV for take-off angles from 20° to 90°. The O 1s peak shifts from 532.9 eV at 20° to 532.5 eV at 40° where it remains fixed up to 90°. The slight shift of the O 1s peak at the near surface is attributed to either adsorbed water or adventitious carbon on the surface.

The morphology of a yttrium silicate film formed by oxidizing ~8 Å of yttrium on silicon at 900 °C for 15 seconds was studied using cross-sectional TEM (Fig. 4). Lattice fringes are detected in the aluminum capping layer and the silicon substrate, but the yttrium silicate layer is free of lattice fringes indicating the amorphous nature of the film. Based on the substrate lattice spacing, the yttrium silicate film is 42 Å thick. The interface between the yttrium silicate and the silicon substrate is sharp with no indication for an interface layer between the two materials.

The C-V curve for a yttrium silicate capacitor on n-type Si(100) with an Al electrode is presented in Fig. 5. The Y-O-Si film was formed by oxidizing an ~8 Å yttrium film on silicon at 900 °C for 15 seconds in 1 atm. N_2O. Analysis of the C-V curve that includes the correction for the quantum confinement of electrons in the semiconductor yields EOT = 12 Å with leakage current of 0.5 A/cm^2 at 1V above the flatband voltage (V_{fb}). A set of approximately 15 samples formed under similar conditions resulted in C-V curves with similar shape and V_{fb}, with EOT values ranging from 10 to 14 Å. Since a thickness of 42 Å is measured for films undergoing the same processing, a

dielectric constant of ~14 is estimated for the yttrium silicate film. The flatband voltage (V_{fb}) is measured at V_{fb} = -0.74 V, which is shifted –0.68 V from the expected V_{fb} for an ideal capacitor.

When a reactive metal is deposited onto silicon and oxidized at elevated temperature, the metal can react with silicon and become oxidized. Consistent with the XPS and MEIS spectra of Figs. 1, 2 and 3, the oxidation of a thin yttrium layer on silicon results in a film with a significant fraction of Y-O-Si bonds. The Y 3d, Si 2p and O 1s (Fig. 1) peak positions for a film formed by oxidizing a thin yttrium layer on silicon are different from those expected for either pure Y_2O_3 or SiO_2 indicating the presence of Y-O-Si bonding structure. The chemical shifts of the Y 3d, Si 2p and O 1s peaks are due to charge transfer from yttrium to neighboring Si-O bonds consistent with the relative electronegativity of yttrium, silicon and oxygen (1.2, 1.8, 3.5 on the Pauling scale). The Y 3d, Si 2p and O 1s spectra do not show clear spectroscopic evidence for phase separated Y_2O_3, SiO_2 or Y-Si. The broadness (FWHM = 3.0 eV) of the O 1s peak is consistent with a combination of oxygen bound to yttrium and oxygen bound to silicon. Analysis of the MEIS spectrum in Fig. 2 yields a composition of $(Y_2O_3)_{0.32}\cdot(SiO_2)_{0.68}$, which is within the experimental error ($x = 0.32 \pm 0.04$) of the known silicate $Y_2Si_2O_7$ ($x = 0.33$). The angle resolved XPS spectra (Fig. 3) indicate that the oxidation of a thin yttrium layer on silicon results in an yttrium silicate film with homogeneous chemical bonding. The constancy as a function of take-off angle of the Y 3d, Si 2p and O 1s peak positions in the angle resolved spectra signifies the consistency of the chemical states within the yttrium silicate film. The Y 3d and Si 2p peaks in yttrium silicate can shift considerably (up to >1.0 eV) when the composition of the film changes[19]. Since angle resolved XPS does not detect any shifting in the Y 3d and Si 2p peaks positions, the yttrium silicate films are of constant composition throughout the depth of the film. The C-V curve of Fig. 5 illustrates the scalability of the yttrium silicate dielectric down to the 10 Å EOT regime. The films in Fig. 5 were formed by the same process as films shown in Figures 1 and 2 above. A sizeable flatband shift suggests the presence of positive fixed charge in a sufficient density to be a concern. The leakage current of 0.5 A/cm^2 is several orders of magnitude less than for a silicon dioxide of equivalent capacitance (J_g ~ 100-1000 A/cm^2).[2] Similar to other high-k dielectrics, the leakage is greater than that expected for a SiO_2 of similar physical thickness (~$1x10^{-9}$ A/cm^2)[20] consistent with a lower tunneling barrier and/or additional current transport pathways in the high-k material.

As discussed in detail elsewhere,[13] the chemical bonding structure of yttrium silicate films formed using the method described here likely results from a competition between yttrium-silicon reaction to form a silicide-like material and oxidation of the yttrium and silicon to form Y-O-Si. The following (unbalanced) reactions are all possible in this materials system:

$$Y\,(s) + O_2\,(g) \rightarrow Y_2O_3\,(s) \qquad \text{(i)}$$

$$Y\,(s) + Si\,(s) \rightarrow YSi\,(s) \qquad \text{(ii)}$$

$$YSi\,(s) + O_2\,(g) \rightarrow Y\text{-}O\text{-}Si\,(s) \qquad \text{(iii)}$$

$$Si\,(s) + O_2\,(g) \rightarrow SiO_2\,(s) \qquad \text{(iv)}$$

$$Y\,(s) + SiO_2\,(s) \rightarrow Y\text{-}O\text{-}Si\,(s) \qquad \text{(v)}$$

While reaction kinetics will favor some of these reactions over others, the results do not clearly identify one rate-limiting step. However, other experiments[13,19] show that the degree of silicon consumption depends on the oxidation temperature and the initial thickness of the yttrium film indicating that reactions (i) and (ii) occur at comparable rates and that reaction (iii) is faster than

reaction (iv). Engineered interfaces can also be implemented to control silicon consumption during oxidation of thin yttrium films[21] and the details are shown below in the following section.

B. Effect of silicon surface pretreatments on silicon incorporation

The consumption of silicon during oxidation of yttrium films was studied using the following pretreatments: (1) bare silicon, (2) oxidized silicon, (3) nitrided-oxidized silicon, and (4) nitrided silicon. All oxidation and nitridation steps were performed *in situ* on bare silicon before yttrium deposition. Figure 6 presents the Si 2p and N 1s spectra of the silicon surface pretreatments before yttrium deposition and oxidation. The silicon substrate peak (99.3 eV) in the Si 2p spectra (Fig. 6a) is clearly visible for each pretreatment. A high binding energy (102-103 eV) feature is observed in the Si 2p spectra for each of the plasma treated surfaces (Fig. 6a.2-4), but not for the bare silicon surface (Fig. 6a.1). The feature at 103.3 eV for the plasma oxidized silicon (Fig. 6a.2) and plasma oxidized silicon followed by nitridation (Fig. 6a.3) is assigned to SiO_2. The feature at 102.4 eV on the plasma nitrided silicon (Fig. 6a.4) surface is assigned to silicon bound to nitrogen. The thickness of the oxidized silicon and nitrided silicon layers was estimated from the attenuation of the Si^O feature to be ~5-10 Å. No detectable nitrogen is observed on the surface of the bare silicon that has been exposed to air (Fig. 6b.1). The N 1s spectra for the plasma oxidized silicon (Fig. 6b.2), plasma oxidized silicon followed by nitridation (Fig. 6b.3) and the plasma nitrided silicon (Fig. 6b.4) all display a nitrogen feature near 398 eV. Nitrogen is observed in the plasma oxidized sample because the oxidation is done using N_2O. The plasma nitrided silicon clearly contains the most nitrogen, and the N 1s feature of the plasma nitrided-oxidized silicon pretreatment is larger (~70%) in area than the N 1s of the plasma oxidized silicon.

Figure 7 presents the Y 3d (Fig. 7a), Si 2p (Fig. 7b) and the O 1s (Fig. 7c) spectra after yttrium deposition and oxidation for experiments (1)-(4). For oxidation of yttrium deposited onto bare silicon (Fig. 7a.1), the Y $3d_{5/2}$ peak is measured at 158.3 eV consistent with a yttrium silicate film. The Y $3d_{5/2}$ peak positions for the films formed on oxidized silicon (Fig. 7a.2) and oxidized silicon with nitridation (Fig. 7a.3) are measured near 158.3 eV, with perhaps slight shifting to lower binding energy for the film formed on the nitrided-oxide. However, when yttrium is deposited on nitrided silicon and oxidized (Fig. 7a.4), the Y $3d_{5/2}$ peak shifts 0.8 eV to lower binding energy compared to the Y 3d position of the yttrium silicate film formed on bare silicon. As the Y 3d peak shifts to lower binding energy, it moves toward the expected peak position for Y_2O_3 (156.8 eV), consistent with an increase in Y-O-Y bond density. A silicon substrate feature at 99.3 eV and a feature at ~102 eV are observed in the Si 2p spectra (Fig. 7b.1-4) for the films formed on each silicon surface pretreatment. The Si 2p spectrum for the film formed on bare silicon (Fig. 7b.1) exhibits a peak at 102.2 eV consistent with an yttrium silicate film. The Si 2p spectra for the films formed on oxidized silicon (Fig. 7b.2) and nitrided-oxidized silicon (Fig. 7b.3) exhibits similar features at ~102 eV. The spectrum for the plasma oxidized silicon from Fig. 6a.2 is reproduced in Fig. 7b.2´ for reference. The feature at 102.0 eV for the film formed on nitrided silicon (Fig. 7b.4) is shifted 0.2 eV toward lower binding energy and is ~50% of the area of the film formed on bare silicon. The O 1s peak at 532.0 eV measured for the yttrium silicate film formed on bare silicon (Fig. 7c.1) is a broad peak resulting from the combined effects of oxygen bound to yttrium and oxygen bound to silicon. Slight shifting of the O 1s peak maximum is observed when comparing the spectra for the films formed on oxidized silicon (Fig. 7c.2), nitrided-oxidized silicon (Fig. 7c.3) and nitrided silicon (Fig. 7c.4) to the spectrum for the film formed on bare silicon (Fig. 7c.1). However, the most pronounced difference between these spectra are the shoulders at ~530.0 eV observed in the O 1s spectrum of the films formed on nitrided-oxidized silicon and nitrided silicon.

The shoulders at ~530.0 eV are near the expected binding energy for O 1s in Y_2O_3 (529.5 eV) and indicate an increase in the O-Y-O bonding in the films.

The results of the MEIS analysis of the films formed on pretreated silicon are presented in Fig. 8. The proton energy spectra for the films formed on bare silicon (Fig. 8.1), oxidized silicon (Fig. 8.2), nitrided-oxidized silicon (Fig. 8.3) and nitrided silicon (Fig. 8.4) all exhibit peaks for yttrium (~96 keV), silicon (~86 keV) and oxygen (~80.5 keV). The small feature near 89 keV is due to argon, incorporated in small amounts in the film during the initial argon sputter deposition of yttrium. The shoulder (~87 keV) on the silicon substrate peak is clearly evident in the spectrum of the yttrium silicate film formed on bare silicon. However, this shoulder is barely evident in the spectrum of the film formed on nitrided silicon indicating less silicon content relative to the yttrium silicate formed on bare silicon. The difference between the silicon content of the yttrium silicate film formed on bare silicon and the film formed on nitrided silicon is clearly indicated in the calculated MEIS depth profiles for these films. As presented in Fig. 9, the silicon distribution is approximately constant at $0.6x10^{22}$ atoms/cm^3 for the yttrium silicate formed on bare silicon (Fig. 9.1), whereas the silicon distribution increases from approximately zero to $0.6x10^{22}$ atoms/cm^3 at a depth of 20 Å for the film formed on nitrided silicon (Fig. 9.4). The film formed on nitrided silicon displays a feature for nitrogen in the proton energy spectrum at ~76.5 keV; this feature is very weak in the raw spectra of the films formed on the oxidized silicon and nitrided-oxidized silicon and below the detection limit (<0.3 monolayer) for the film formed on bare silicon. The depth profile for the film formed on nitrided silicon (Fig. 9.4) indicates that $1.1x10^{15}$ atoms/cm^2 areal density of nitrogen remains localized at the interface after yttrium deposition and oxidation.

The XPS and MEIS results (Figs. 7-9) demonstrate the effects that oxygen and nitrogen silicon surface pretreatments have on silicon consumption during oxidation of deposited yttrium. When yttrium is deposited onto silicon and oxidized (experiment "1" in Figs. 7-9), the chemical shifts of the Y 3d, Si 2p and O 1s peaks (Fig. 7.1) are consistent with a film with a significant fraction of Y-O-Si bonds. This bonding structure likely results from the high reactivity of the yttrium metal contributing to concurrent silicide and oxidation reactions, leading to silicate. The peak (~87 keV) for silicon in the film is clearly largest for the films formed on bare silicon. The composition of this film is $(Y_2O_3)_{0.58}\cdot(SiO_2)_{0.42}$ consistent with yttrium orthosilicate (Y_2SiO_5) containing ~28% Y_2O_3. Phase separated Y_2O_3 is not detected at 156.8 eV in the XPS spectra, perhaps due to dispersal of Y_2O_3 groups within the silicate bulk or bond strain in Y_2O_3 clusters.

Similar results are observed in the XPS and MEIS (Figs. 7.2-3 and 8.2-3) results for experiments (2) and (3) where yttrium is deposited on oxidized silicon and nitrided-oxidized silicon, respectively, and the stacks are then oxidized. Films formed by the oxidation of yttrium on an oxidized silicon pretreatment contain considerable amounts of Y-O-Si bonding, although the film formed on nitrided-oxidized silicon contains less silicon than the films formed on bare and oxidized silicon. The Y 3d, Si 2p and O 1s results for both cases are similar to the yttrium silicate film formed on bare silicon. However, more O-Y-O bonding is observed in the O 1s spectra for the film formed on nitrided-oxidized silicon. The composition of the film formed on oxidized silicon is $(Y_2O_3)_{0.63}\cdot(SiO_2)_{0.37}$, which is indistinguishable from the yttrium silicate formed on bare silicon (experimental error $x \pm 0.04$), and the composition of the film formed on nitrided-oxidized silicon is $(Y_2O_3)_{0.72}\cdot(SiO_2)_{0.28}$ indicating that the silicon fraction is reduced compared to the film formed on bare silicon. The spectrum for the oxidized silicon pretreatment is presented as a reference in Fig. 7.b. (spectrum 2´). The Si 2p spectra for the films formed on oxidized silicon and nitrided-oxidized silicon are consistent with a reduction in SiO_2 concentration after yttrium deposition and oxidation.

When subjected to an oxidizing ambient at elevated temperature, yttrium deposited on a SiO_2 layer will react with the silicon oxide to form a silicate, as discussed in detail in Section III.C. However, when yttrium is deposited on a nitrided-oxidized silicon film (experiment "3"), the yttrium consumes the interfacial SiO_2 and the interfacial nitrogen impedes consumption of silicon resulting in a slightly reduced silicon fraction.

When the silicon surface is nitrided prior to yttrium deposition and oxidation (experiment "4"), the XPS and MEIS results indicate a significantly reduced silicon content compared to the yttrium silicate film formed on bare silicon. As a result of the decreased silicon fraction in the film, the Y 3d peak for the film formed on nitrided silicon is shifted toward more Y_2O_3-like bonding, the O 1s peak exhibits a definite shoulder near the expected O 1s position for Y_2O_3, and the MEIS peak for silicon in the film is diminished. The composition determined from MEIS is $(Y_2O_3)_{0.79}\cdot(SiO_2)_{0.21}$, which corresponds to a Y_2O_3 film with ~27% yttrium silicate. The MEIS depth profile for the film formed on nitrided silicon demonstrates that the nitrided interface has remained intact after yttrium deposition and oxidation. The interfacial nitrogen is responsible for reducing the consumption of silicon by providing a silicon diffusion barrier that impedes the reaction between yttrium and silicon and allows formation of Y_2O_3.

The inter-diffusion of silicon and some metals, including Y, Hf, Zr and La, to form silicides at relatively low temperatures is a well-known phenomenon.[22,23] When yttrium (which forms a silicide and stable oxide) on silicon is oxidized (experiment "1"), the above results indicate that yttrium and silicon react and oxidize to form yttrium silicate. Similar films are observed when the silicon surface is pre-oxidized before yttrium deposition and oxidation (experiments "2" and "3"). When the silicon surface is oxidized and nitrided prior to yttrium deposition (experiment "3"), the silicate formation reaction is somewhat impeded during oxidation. The yttrium can react with the SiO_2, but further reaction with the silicon substrate is inhibited. However, when the silicon surface is nitrided *without oxidation* prior to yttrium deposition (experiment "4"), the reaction between yttrium and silicon during oxidation is significantly impeded, resulting in an Y_2O_3 film with a small fraction (~27%) of silicate bonding. Recently, nitrided oxide and silicon nitride films have been used as diffusion barriers to reduce boron penetration into the gate oxide.[24,25] It is reasonable to assume that the silicon nitride pretreatment described in this work provides a sufficient silicon diffusion barrier to suppress the reaction between the yttrium and silicon.

C. Consumption of SiO_2 by yttrium

Reaction between yttrium and SiO_2 to form yttrium silicate was postulated to explain the consumption of silicon by yttrium in experiments (2) and (3) in Section III.B. Yttrium films (25 Å) on thermal SiO_2 (40 Å) were subjected to oxidizing or vacuum annealing (~10^{-6} Torr) conditions and probed using XPS to confirm the conversion of SiO_2 to yttrium silicate. Figure 10 presents XPS results for the oxidation of yttrium films on SiO_2 at 600 and 900 °C in 1 atm. N_2O for 2 minutes. The spectra of the 40 Å SiO_2 film prior to yttrium deposition and oxidation is presented in Fig. 10 as a reference. The Y $3d_{5/2}$ peaks (Fig. 10a) for the films after oxidation at 600 and 900 °C are measured at 158.8 and 159.2 eV, respectively, consistent with Y-O-Si bonding. The spectrum for oxidation at 600 °C exhibits blurring of the spin-orbit splitting indicating the presence of multiple yttrium oxidation states. The Si 2s peaks for SiO_2 are visible in the Y 3d window at 154.9 and 150.6 eV for the Si-O and substrate peaks, respectively. The silicon substrate peak (99.3 eV) is observed in the Si 2p spectra (Fig. 10b) for SiO_2 and for the films after oxidation of yttrium on SiO_2. The Si-O peak is measured at 103.6 eV for SiO_2 and at 102.9 eV for the films after oxidation of yttrium on SiO_2. The Si-O feature for the films after oxidation of yttrium on silicon are consistent with yttrium

silicate and do not exhibit evidence for SiO_2 (within detectable limits). Consistent with an increase in overlayer thickness, the silicon substrate and Si-O peaks for the films after yttrium deposition and oxidation are attenuated relative to the original SiO_2 layer. The Si-O peaks for the films after yttrium deposition and oxidation are broader (FWHM = 2.2 eV) compared to the Si-O peak for SiO_2 (FWHM = 1.8 eV) consistent with a wider range of bonding configurations for silicon in the films after yttrium deposition and oxidation. The Si-O feature for the film oxidized at 600 °C is 50% smaller in area than the Si-O feature of the film oxidized at 900 °C. The O 1s peaks (Fig. 10c) for yttrium/SiO_2 oxidized at 600 °C, yttrium/SiO_2 oxidized at 900 °C and SiO_2 are measured at 532.7, 532.4 and 533.5 eV, respectively. The FWHM for yttrium/SiO_2 oxidized at 600 °C, yttrium/SiO_2 oxidized at 900 °C and SiO_2 are 3.4, 2.4 and 1.8 eV, respectively. The O 1s peaks for the films after yttrium deposition and oxidation are broad peaks consistent with the combination of oxygen bound to yttrium and silicon. The O 1s peak for yttrium on SiO_2 oxidized at 600 °C displays asymmetry on the low binding energy side of the peak consistent with O-Y-O bonding. Figure 11 presents the XPS results for yttrium on SiO_2 annealed at 600 °C in vacuum for 2 minutes. Again, the spectrum for the 40 Å SiO_2 is presented as a reference. The Y $3d_{5/2}$ (Fig. 11a), Si-O Si 2p (Fig. 11b) and O 1s (Fig. 11c) peaks for yttrium on SiO_2 annealed in vacuum are measured at 158.2, 102.0 and 531.7 eV similar to the peaks for the yttrium film on SiO_2 oxidized at 600 and 900 °C. The Si-O feature (FWHM = 2.3 eV) for the yttrium on silicon annealed in vacuum does not exhibit any evidence for SiO_2. The O 1s peak is a broad peak (FWHM = 3.1 eV) resulting from oxygen bound to yttrium and silicon.

The spectra of Figs. 10 and 11 confirm the reaction between SiO_2 and Y to form yttrium silicate under oxidizing or vacuum annealing conditions. When yttrium on SiO_2 is oxidized or vacuum annealed, the Y 3d, Si 2p and O1s peak positions are consistent with Y-O-Si bonding, with only subtle differences between films formed on Si or SiO_2. The yttrium film on SiO_2 oxidized at 900 °C (Fig. 10) is similar to the yttrium silicate film formed by oxidation of yttrium on silicon at 900 °C (Fig. 1). The yttrium film on SiO_2 annealed in vacuum at 600 °C (Fig. 11) has structure similar to the yttrium silicate film formed by oxidation of yttrium on silicon at 600 °C (Fig. 7.1), since the spectra for both films are similar in shape and position. Although the spectra of the film formed by oxidizing yttrium on SiO_2 at 600 °C (Fig. 10) indicate a significant fraction of Y-O-Si bonding, the blurring of the Y 3d spin-orbit spitting, the reduced Si-O feature size and the broadness of the O 1s feature suggest the presence of some Y_2O_3-like bonding. When yttrium on SiO_2 is exposed to an oxidizing ambient, there exists a competition between oxidation of the yttrium (reaction "i" in the scheme presented in Section III.A) and consumption of the SiO_2 (reaction "v"). Perhaps, the reaction between yttrium and SiO_2 during oxidation at 600 °C does not completely consume the yttrium leaving metal available for oxidation to Y_2O_3. In any case, there is enough evidence in Fig. 10 for Y-O-Si bonding (i.e. binding energy of Y $3d_{5/2}$, Si-O Si 2p and O 1s) to conclude that the yttrium has converted some of the SiO_2. These results contrast a previous study where zirconium thin films on SiO_2 were annealed in vacuum and a $ZrO_2/Zr_5Si_4/SiO_2$ multi-layered structure formed.[26] In the Zr/O/Si system, the oxygen content of the mixed zirconium and silicon layer could not be determined by Rutherford backscattering due to overlap of the oxygen signal from the SiO_2 substrate. However, the reported formation of ZrO_2 is distinctly different from the observed formation of yttrium silicate discussed here suggesting significantly different kinetic pathways in the group IIIB and IVB metal oxide systems. The results presented here are in agreement with the ionized cluster beam growth of Y_2O_3 where a thin layer of yttrium is deposited on a SiO_2 substrate at 500 °C before being exposed to oxygen, which results in an amorphous SiO_x layer that can be

attributed to a Y-O-Si film.[3] Since the free energy of formation for Y_2O_3 ($-\Delta G_f$ = 434.0 kcal/mol at 25 °C) is greater than for SiO_2 ($-\Delta G_f$ = 204.6 kcal/mol at 25 °C), yttrium can reduce silicon with Y_2O_3 and Si being the expected products.[12] However, the XPS results of Fig 11 indicates the conversion of SiO_2 to yttrium silicate. The lack of thermodynamic data for $Y_2Si_2O_7$ and Y_2SiO_5 prevents complete evaluation of the (unbalanced) reaction $Y + SiO_2 + O_2 \rightarrow (Y_2Si_2O_7$ or $Y_2SiO_5)$ to determine if the silicates are energetically favorable products. However, previous researchers have measured the enthalpy of formation ($-\Delta H_f$) for Y_2SiO_5 as $-\Delta H_f$ (25 °C) = 685.3 kcal/mol.[27] The experiments described here are performed at relatively moderate temperatures (600-900 °C) with no phase changes. Under these conditions, the entropy change can be considered negligible, and ΔG_f can be approximated as $\Delta G_f \cong \Delta H_f$, (since $\Delta G = \Delta H - T\Delta S$, where T is the temperature and ΔS is the entropy change). For the reaction $2Y + SiO_2 + 3/2\ O_2 \rightarrow Y_2SiO_5$, $\Delta G_f \cong \Delta H_f$ = -480.7 kcal/mol, which implies that the formation of yttrium silicate is thermodynamically favorable. This processes provides an interesting method to convert the existing SiO_2 gate dielectric to a high-k dielectric in a straightforward manner using thermal oxidation of silicon followed by metal deposition, annealing and re-oxidation.

IV. Conclusions

Interface bulk bonding structure during oxidation of ultra-thin metal and metal silicide thin films on silicon can be controlled by in-situ surface pretreatment steps. When yttrium is deposited onto a bare silicon surface and oxidized, silicon from the substrate is consumed, resulting in an amorphous film that contains predominantly Y-O-Si bonds. MEIS results indicate a graded yttrium concentration, with composition approaching SiO_2 at the interface. XPS, TEM and electrical results do not show clear evidence for interfacial SiO_2, suggesting that more detailed analysis is required to unambiguously determine interface bonding composition. Oxidation of the silicon surface prior to yttrium deposition and oxidation results in an yttrium silicate film similar to the films formed on bare silicon. Oxidizing yttrium on a clean silicon surface exposed only to pre-nitridation results in a structure close to pure metal oxide, consistent with impeded silicon diffusion through the nitrided layer. Conversion of SiO_2 to yttrium silicate is demonstrated for both oxidation and vacuum annealing of yttrium on silicon dioxide. The silicon consumption reactions reported here for the case of yttrium are expected for other metals that form silicides and stable oxides on silicon including Hf, Zr, La, etc. Initial experiments with PVD zirconium on Si and SiO_2 show reactions similar to those observed for yttrium.

Acknowledgments

The authors gratefully acknowledge support from the SRC/SEMATECH Center for Front End Processes and NSF CTS – 0072784.

References

1 S. I. Association, The International Technology Roadmap for Semiconductors, 1999 edition (Austin, TX, 1999).

2 D. A. Buchanan and S.-H. Lo, "Reliability and integration of ultra-thin gate dielectrics for advanced CMOS"; *Microelectronic Engineering* **36,** 13 (1997).

3 D.-H. Lee, T.-Y. Seong, M.-H. Cho, and C.-N. Whang, "Transmission electron microscope structural study of Y_2O_3 films grown on Si(111) substrates by ultrahigh vacuum ionized cluster beam"; *J. Electrochem. Soc.* **146,** 3028 (1999).

4 K.-A. Son, A. Y. Mao, B. Y. Kim, F. Liu, E. D. Pylant, D. A. Hess, J. M. White, D. L. Kwong, D. A. Roberts, and R. N. Vrtis, "Ultrathin Ta2O5 film growth by chemical vapor deposition of Ta(N(CH3)2)5 and O2 on bare and SiOxNy-passivated Si(100) for gate dielectric applications"; *J. Vac. Sci. Technol. A* **16,** 1670 (1998).

5 B. He, T. Ma, S. A. Campbell, and W. L. Gladfelter, "A 1.1 nm oxide equivalent gate insulator formed using TiO2 on nitrided silicon"; *Tech. Dig. Int. Electron Devices Meet.***,** 1038 (1998).

6 M. Balog, M. Schieber, S. Patai, and M. Michman, "Thin films of metal oxides on silicon by chemical vapor depositoin with organometallic compounds"; *J. Cryst. Growth* **17,** 298 (1972).

7 J. Shappir, A. Anis, and I. Pinsky, "Investigation of MOS capacitor with thin ZrO2 layers and various gate materials for advanced DRAM applications"; *IEEE Trans. Electron Devices* **ED-33,** 442 (1986).

8 L. Manchanda, W. H. Lee, J. E. Bower, F. H. Baumann, W. L. Brown, C. J. Case, R. C. Keller, Y. O. Kim, E. J. Laskowski, M. D. Morris, R. L. Opila, P. J. Silverman, T. W. Sorsch, and G. R. Weber, "Gate quality doped high k films for CMOS beyond 100 nm: 3-10 nm Al2O3 with low leakage and low interface states"; *Tech. Dig. Int. Electron Devices Meet.***,** 605 (1998).

9 G. B. Alers, D. J. Werder, Y. Chabal, H. C. Lu, E. P. Gusev, E. Garfunkel, T. Gustafsson, and R. S. Urdahl, "Intermixing at the tantalum oxide/silicon interface in gate dielectric structures"; *Applied Physics Letters* **73,** 1517-1519 (1998).

10 S. K. Kang, D. H. Ko, E. H. Kim, M. H. Cho, and C. N. Whang, "Interfacial reactions in the thin film Y2O3 on chemically oxidized Si(100) substrate systems"; *Thin Solid Films* **353,** 8-11 (1999).

11 T. M. Klein, D. Niu, W. S. Epling, W. Li, D. M. Maher, C. C. Hobbs, R. I. Hegde, I. J. R. Baumvol, and G. N. Parsons, "Evidence of aluminum silicate formation during chemical vapor deposition of amorphous Al2O3 thin films on Si(100)"; *Applied Physics Letters* **75,** 4001-4003 (1999).

12 I. Barin, Thermochemical Data of Pure Substances (VCH Verlagsgesellschaft, Weinheim, Germany, 1989).

13 J. J. Chambers and G. N. Parsons, *Journal of Applied Physics*, in press

14 E. P. Gusev, H. C. Lu, T. Gustafsson, and E. Garfunkel, "Growth-Mechanism of Thin Silicon-Oxide Films On Si(100) Studied By Medium-Energy Ion-Scattering"; *Physical Review B-Condensed Matter* **52,** 1759-1775 (1995).

15 J. F. Ziegler and J. P. Biersack, SRIM-The Stopping and Range of Ions in Matter, Vol. 9 (IBM, 1998).

16 Q. Yang, D. J. O'Connor, and Z. Wang, ; *Nucl. Inst. Meth.* **B61,** 149 (1991).

17 E. M. Levin, C. R. Robbins, and H. F. McMurdie, Phase Diagrams for Ceramists: 1969 Supplement, Vol. Figure 2388 (The American Ceramic Society, Columbus, Ohio, 1969).

18 J. F. Moulder, W. F. Stickle, P. E. Sobol, and K. D. Bomben, Handbook of X-ray Photoelectron Spectroscopy (Perkin-Elmer Corporation, Eden Prairie, MN, 1992).

19 J. J. Chambers and G. N. Parsons, to be published

20 K. H. Lee and S. A. Campbell, "The kinetics of oxide charge trapping and breakdown in ultrathin silicon dioxide"; *J. Appl. Phys.* **73,** 4434 (1993).

21 J. J. Chambers and G. N. Parsons, "Yttrium silicate formation on silicon: Effect of silicon preoxidation and nitridation on interface reaction kinetics"; *Appl. Phys. Lett.* **77,** 2385 (2000).

22 J. E. E. Baglin, F. M. d'Heurle, and C. S. Petersson, "Diffusion Marker Experiments With Rare-Earth Silicides and Germanides - Relative Mobilities of the 2 Atom Species"; *Journal of Applied Physics* **52,** 2841-2846 (1981).

23 A. Pellissier, R. Baptist, and G. Chauvet, "Mechanism of the Y/Si Interface Formation Studied By Photoemission"; *Surface Science* **210,** 99-113 (1989).

24 M. Navi and S. T. Durham, "Effect of film density on boron diffusion in SiO2"; *Appl. Phys. Lett.* **72,** 2111 (1998).

25 Y. Wu, H. Niimi, H. Yang, G. Lucovsky, and R. B. Fair, "Suppression of boron transport out of p+ polycrsystalline silicon at polycrystalline silicon dielectric interfaces"; *J. Vac. Sci. Technol. B* **17,** 1813 (1999).

26 S. Q. Wang and J. W. Mayer, "Reactions of Zr thin films with SiO2 substrates"; *J. Appl. Phys.* **64,** 4711 (1988).

27 J.-J. Liang, A. Navrotsky, T. Ludwig, H. J. Seifert, and F. Aldinger, "Enthalpy of formation of rare-earth silicates Y2SiO5 and Yb2SiO5 and N-containing silicate Y10(SiO4)6N2"; *J. Mater. Res.* **14,** 1181 (1999).

Figure Captions

Fig. 1. The Y 3d (a), Si 2p (b), and O 1s (c) regions of the XP spectra for an yttrium silicate film formed by oxidation of an ~8 Å yttrium film on silicon at 900 °C for 15 seconds. The chemical shifts of the Y 3d, Si 2p and O 1s peaks are consistent with a significant fraction of Y-O-Si bonding in the film.

Fig. 2. (a) MEIS spectrum for an yttrium silicate film formed by oxidation of an ~8 Å yttrium film on silicon at 900 °C for 15 seconds. Near surface silicon is detected as the shoulder (~87 keV) on the silicon substrate peak. (b) Corresponding depth profile. The composition of this film determined from the fitting is $(Y_2O_3)_{0.32}\cdot(SiO_2)_{0.68}$. Due to uncertainty in the proton energy loss straggling, the yttrium profile lies within the two extreme profiles labeled as (i) and (ii).

Fig. 3. Angle resolved XPS of the Y 3d (a), Si 2p (b) and O 1s (c) regions for an yttrium silicate film formed by oxidation of a ~25 Å yttrium film on silicon at 900 °C for 2 minutes. No interface layer can be discerned, and the chemical states are consistent throughout the film.

Fig. 4. Cross-sectional TEM image of an yttrium silicate film formed by oxidation of an ~8 Å yttrium film on silicon at 900 °C for 15 seconds. The film appears amorphous with no interface layer.

Fig. 5. Typical 1 MHz C-V curve for an Al/Y-O-Si/n-type capacitor. The yttrium silicate was formed by oxidation of an ~8 Å film on silicon at 900 °C for 15 seconds. The yttrium silicate film has an equivalent oxide thickness of 12 Å.

Fig. 6 Si 2p (a) and N 1s (b) spectra for the silicon surface pretreatments used in this study: (1) bare silicon, (2) plasma oxidized silicon, (3) plasma nitrided-oxidized silicon, and, (4) plasma nitrided silicon. The thickness of the plasma surface treatments is estimated using the attenuation of the silicon substrate peak as 5-10 Å.

Fig. 7. Y 3d (a), Si 2p (b) and O 1s (c) regions of the XP spectra for the yttrium silicate films formed on: (1) bare silicon, (2) plasma oxidized silicon, (3) plasma nitrided-oxidized silicon, and, (4) plasma nitrided silicon. The spectra of the films formed on (1)-(3) are consistent with Y-O-Si bonding. The film formed on (4) has significantly more Y-O-Y bonding than the films formed on (1)-(3), as denoted by the shift of the Y 3d peak and the shoulder on the O 1s peak.

Fig. 8. MEIS spectra for the yttrium silicate films formed on: (1) bare silicon, (2) plasma oxidized silicon, (3) plasma nitrided-oxidized silicon, and, (4) plasma nitrided silicon. The shoulder (~87 keV) on the silicon substrate peak represents silicon in the film. The yttrium silicate film formed on (1) has the highest silicon fraction and the yttrium silicate film formed on (4) has the lowest silicon fraction of the films tested.

Fig. 9. Calculated MEIS depth profiles for the yttrium silicate films formed on (1) bare silicon and (4) nitrided silicon. The profile for the yttrium silicate film formed on (4) clearly exhibits the interfacial nitrogen.

Fig. 10. Y 3d (a), Si 2p (b) and O 1s (c) spectra for a 40 Å SiO_2 and ~25 Å yttrium films on 40 Å SiO_2 oxidized at 600 and 900 °C for 2 minutes. The Y 3d, Si 2p and O 1s peak

positions are consistent with Y-O-Si bonding indicating the conversion of SiO_2 to a silicate.

Fig. 11. Y 3d (a), Si 2p (b) and O 1s (c) spectra for a 40 Å SiO_2 and a ~25 Å yttrium film on 40 Å SiO_2 annealed in vacuum at 600 °C for 2 minutes. The Y 3d, Si 2p and O 1s peak positions are consistent with Y-O-Si bonding indicating the conversion of SiO_2 to a silicate.

Figure 1. J. J. Chambers

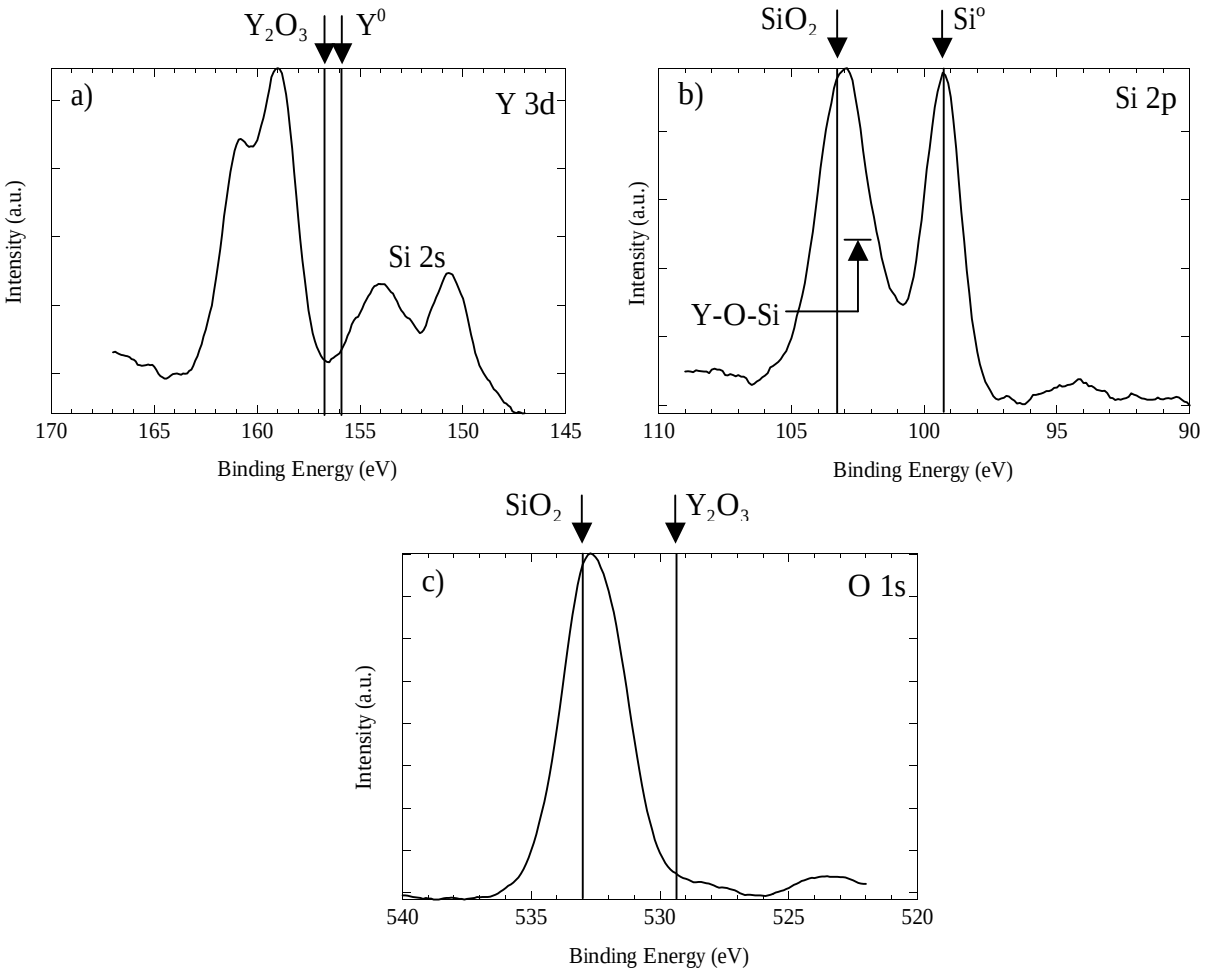

Figure 2. J. J. Chambers

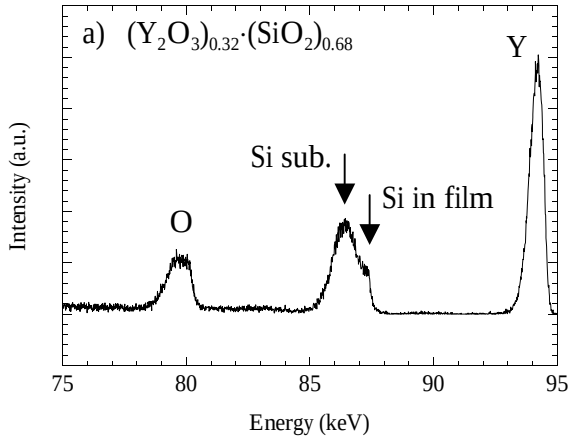

Figure 2b.

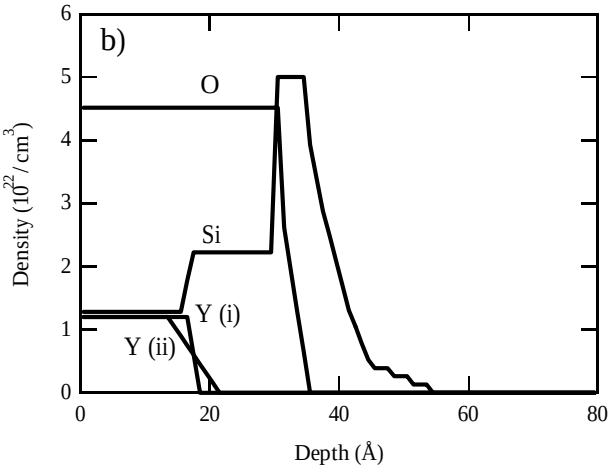

Figure 3. J. J. Chambers

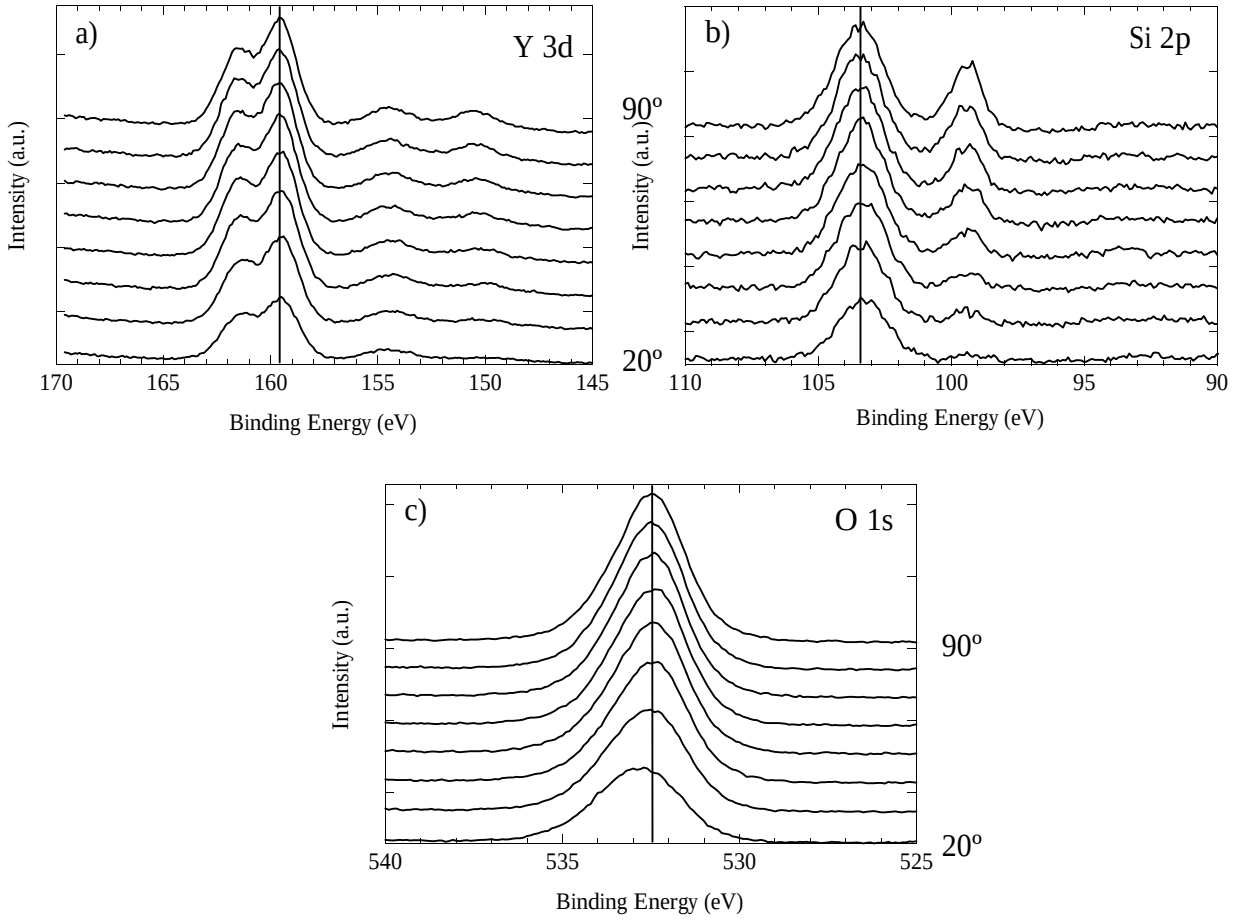

Figure 4. J. J. Chambers

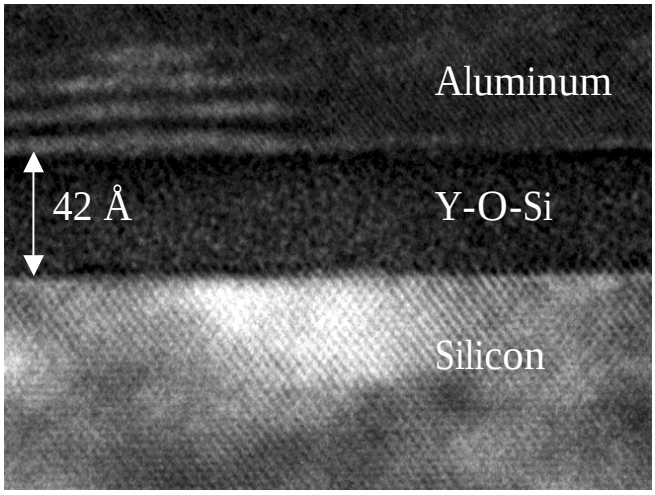

Figure 5. J. J. Chambers

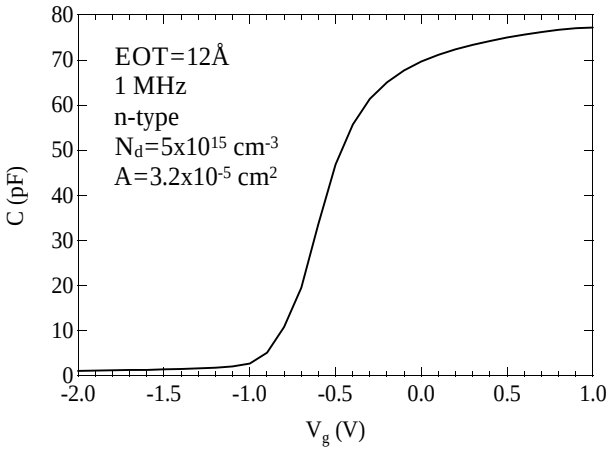

Figure 6. J. J. Chambers

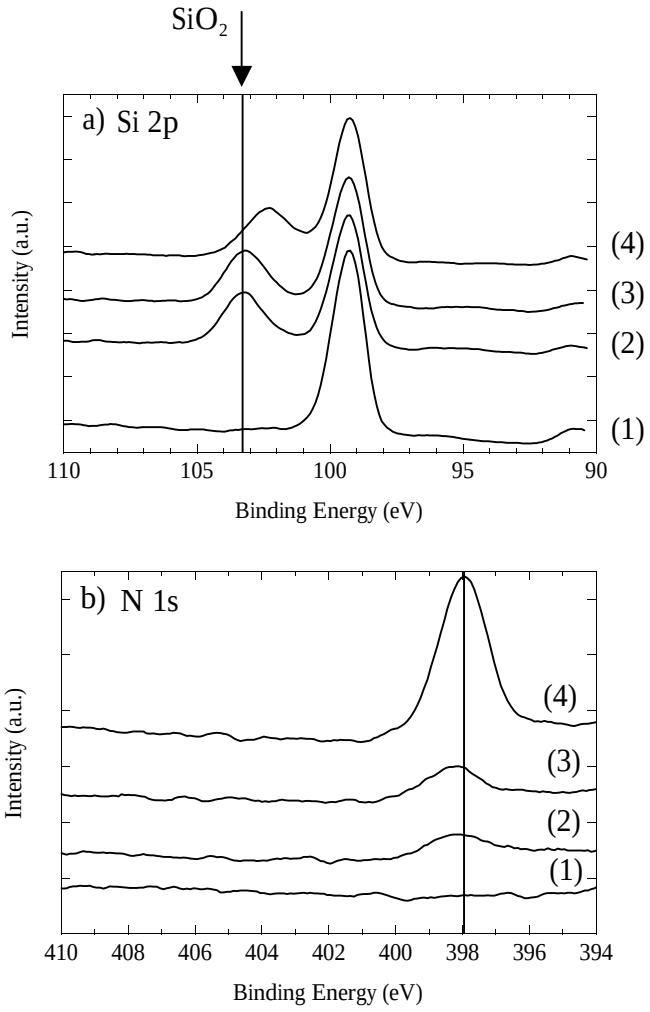

Figure 7. J. J. Chambers

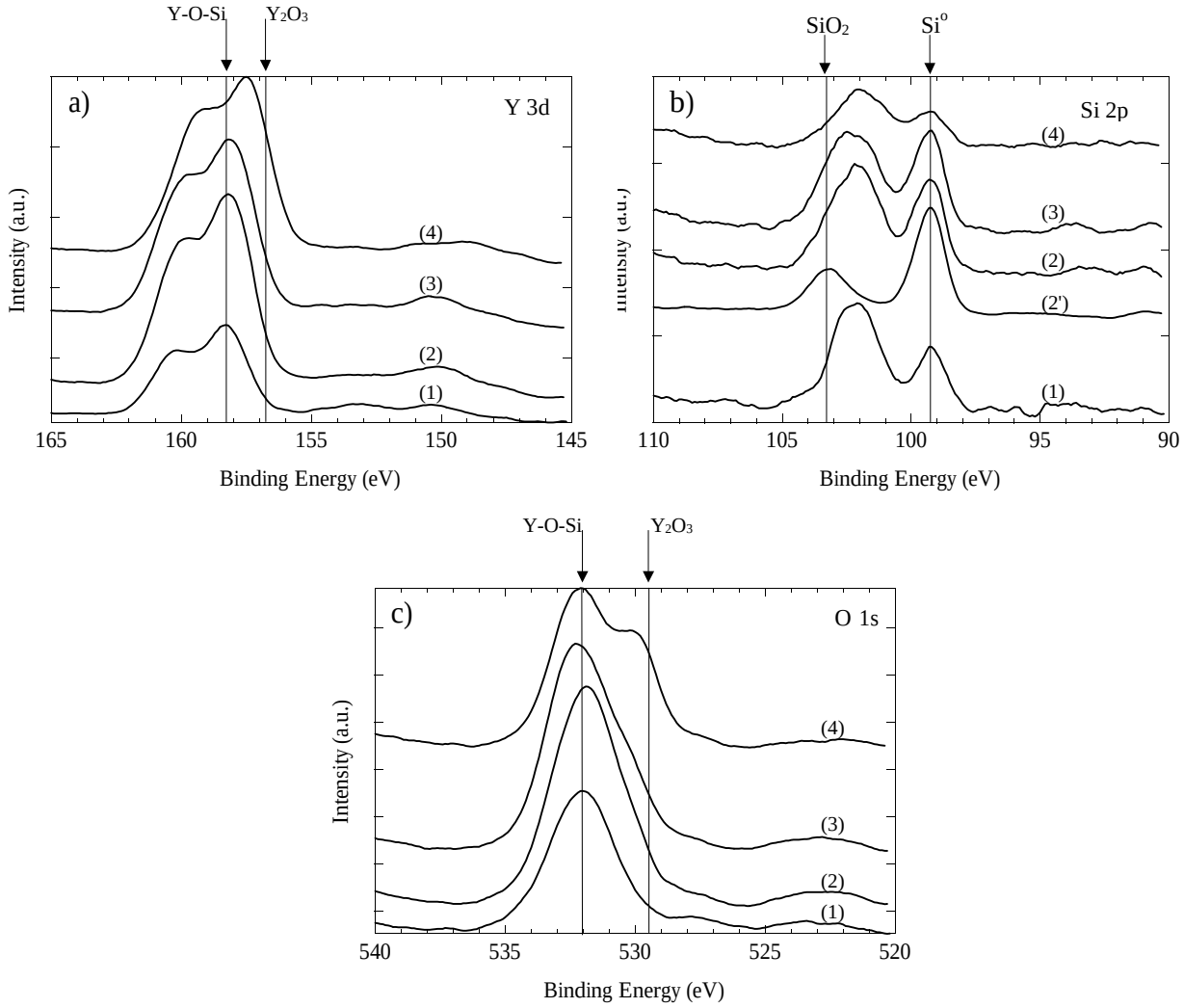

Figure 8. J. J. Chambers

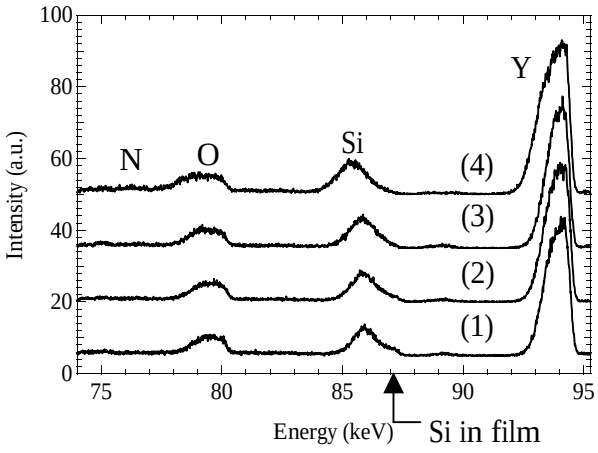

Figure 9. J. J. Chambers

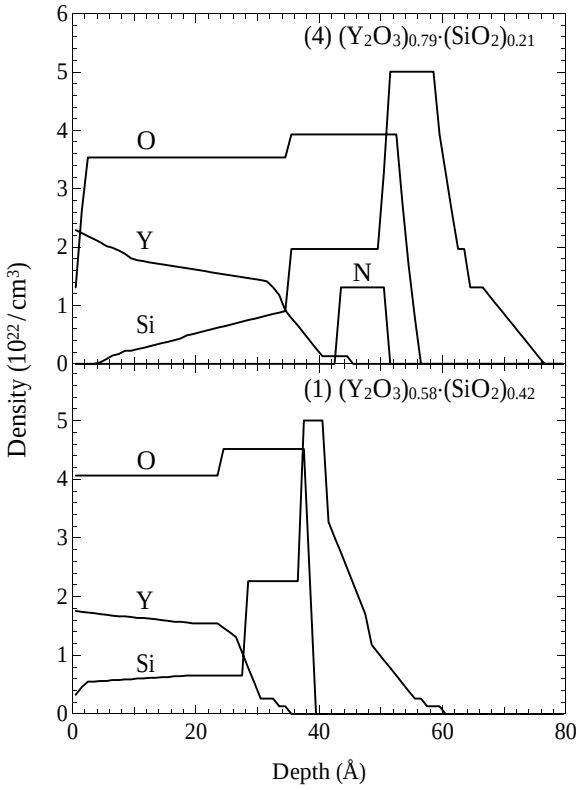

Figure 10. J. J. Chambers

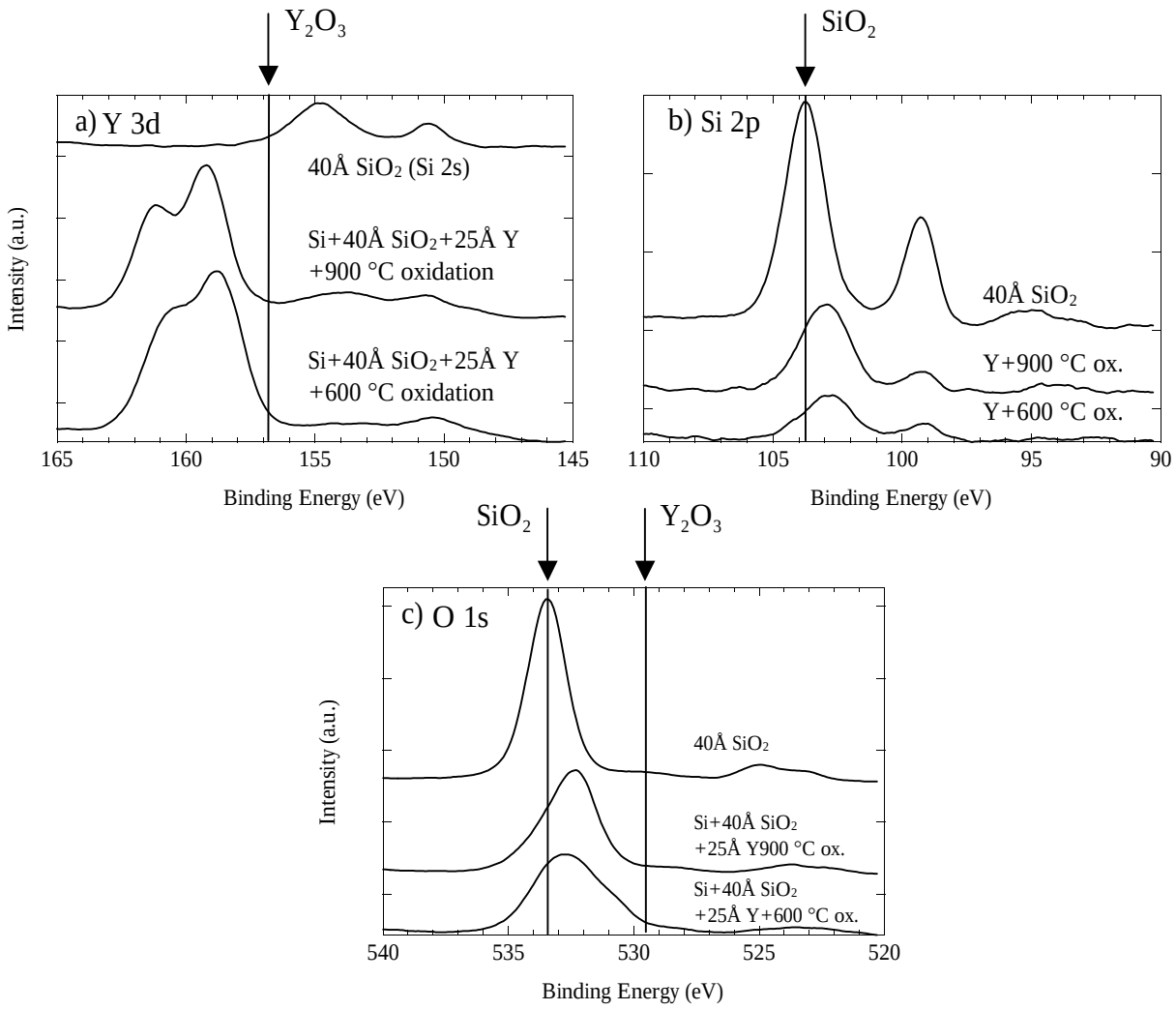

Figure 11. J. J. Chambers